Reduction of the uncertainty of flood hazard analyses under a future climate by integrating multiple SSP-RCP scenarios

Y. Kimura[1,2], Y. Hirabayashi[3], D. Yamazaki[2]

[1]Data Analytics Department, MS&AD InterRisk Research & Consulting, Inc. , 2-105, Kanda Awajicho, Chiyoda-ku, Tokyo 101-0063, Japan
[2]Institute of Industrial Science, The University of Tokyo, 4-6-1 Komaba, Meguro-ku, Tokyo, 153-8505, Japan
[3]Department of Civil Engineering, Shibaura Institute of Technology, 3-7-5 Toyosu, Koto-ku, Tokyo, 135-8548, Japan

Correspondence to: Y. Kimura (yu1590yu@gmail.com)

Abstract. The uncertainty due to small number of ensemble members is a major source of uncertainty in future climate predictions. While the uncertainty due to the above in general circulation models (GCMs) projections can be mitigated by increasing the number of simulation ensembles, only a limited number of large-ensemble experiments are available in CMIP6 future scenario experiments. Here we propose a method that increases the sample ensemble size in evaluations of future hazard, by integrating multiple SSP-RCPs for a time period corresponding to a specific increase in temperature from the preindustrial level (i.e., X°C warming). The success of the method was assessed by investigating whether the uncertainty due to small number of ensemble members could be reasonably reduced. First, the similarity in the spatial distributions of flood hazard projection at the same warming level was determined for different SSP-RCP scenarios. Under a 2°C warming, all SSP-RCPs had a similar distribution with respect to the change ratio of the flood magnitude. Additionally, we showed that the uncertainty due to the different SSP-RCPs (5%–10%) was smaller than the differences between different warming levels such as between 2°C and 3°C (around 20%–30%), which suggests that differences among SSP-RCPs as to future flood discharge change are relatively small. These results suggested that integrating SSP-RCPs to increase the ensemble size was a reasonable approach, reducing unbiased variance among GCMs in about 70% of land grid points comparing to the result using SSP5-RCP8.5 alone.

1 Introduction

Internal climate variability is a major source of uncertainty in future climate predictions. Indeed, the ability of the El Niño Surthern Occilation and other climate variabilities to influence natural hazard occurrences and disaster impact distribution is well established. The spatial distribution of hazards related to factors such as precipitation varies greatly due to internal variability (Piao et al., 2021; Dai et al., 2019; Wood and Ludwig 2020). In the case of El Niño, it affects the spatiotemporal pattern of flood hazard characteristics on a global scale (Ward et al., 2016). Moreover, internal climate variability also influences climate impact projections (Schwarzwald et al., 2022). Lehner et al., 2020 showed that internal variability is an

issue in future climate change assessments, particularly in the first-decade predictions, when it becomes a dominant factor worldwide. In addition to the internal variability of the climate, the nonlinear response of the atmosphere and ocean, where even slightly different initial values can alter the results, is a major uncertainty in the ensemble's projection results. In order to clarify the range of these uncertainties, studies have included long-term climate simulations (e.g., several thousand years) and numerous ensemble experiments with the same boundary conditions.

Specifically, several studies have indicated that projection uncertainty in general circulation models (GCMs) can be mitigated by increasing the number of ensembles. Shiogama et al., 2023 showed that, for models of precipitation and temperature, increasing the number of ensembles can reduce the uncertainty of GCMs. Maher et al., 2021 also found that large ensembles can separate the effects of the uncertainty in GCMs from those of external forcing. Many studies have evaluated uncertainties in precipitation and flood hazard, using the results of large-ensemble simulations based on multi-year atmospheric and terrestrial data from the Policy Decision-making for Future Climate Change (d4PDF, Mizuta et al., 2017) (Kita and Yamazaki 2023; Ishii and Mori 2020; Cheng et al., 2021). For example, using the d4PDF data, Kita and Yamazaki et al., 2023 mentioned that a small number of ensembles could produce large uncertainty, especially for the severe rainfall and severe floods.

However, studies that have used the Scenario Model Intercomparison Project (ScenarioMIP, O'Neill et al. 2016), the core future projection experiment of Coupled Model Intercomparison Project Phase 6 (CMIP6, Eyring et al., 2016), which are used as the most fundamental data for climate change response, are problematic because there are few GCMs that include large ensembles. Some studies that have used CMIP5 or 6 (Dankers et al., 2014; Brêda et al., 2020; Hirabayashi et al., 2021) have focused on specific time periods, such as the end of the 21st century, but the lack of ensembles inevitably leads to large uncertainties. For example, Hirabayshi et al., 2021 examined future flood risk and associated uncertainty, but the variability in projections among GCMs was still large. The uncertainties were related to differences in the physical processes of the GCMs, to internal climate variability and small number of ensemble members. The use of a larger ensemble for each GCM would reduce the uncertainty in future projections.

To address this problem, here we proposed a method that increases the ensemble sample size in evaluations of future hazards, by integrating multiple SSP-RCPs over the period of a specific temperature rise from preindustrial level (i.e., X°C warming). Because each SSP-RCP has a different range of temperature rise for use in risk assessments for specific time periods, such as the end of the 21st century, different SSP-RCPs should be treated as different sample sets. However, if the spatial patterns of changes in hazards at X°C warming can be considered similar among SSP-RCPs, then the different SSP-RCP scenarios can be considered to make up one sample set. In that case, data integration among SSP-RCPs will increase the sample size and thus reduce uncertainty due to extreme values and the small number of ensemble members of the GCMs. While many studies have evaluated the impact of X°C warming (e.g., Dottori et al., 2018; Alferi et al., 2017), only a few have focused on uncertainty reduction through SSP integration.

This study investigated whether the above projection uncertainty could be reduced by merging multiple SSPs and extracting the periods with the same warming level under each SSP. Precipitation, particularly daily maximum precipitation,

is a major source of uncertainty in climate change projections (Shiogama et al., 2023), such that projections for flood hazard are subject to even greater uncertainty. Thus, we focused on flood hazard, specifically river discharge, and investigated the uncertainty of GCMs. First, we determined whether the distribution of changes in flood hazard among different SSP-RCPs is similar and thus whether integrating SSP-RCPs to increase the ensemble size is justified; then we quantified the extent to which uncertainty can be reduced by our proposed method, which integrates SSP-RCPs.

2 Data and Methods

Both runoff data from GCMs in CMIP6 and a river model were used to investigate the potential reduction in the uncertainties due to small numbers of ensemble members by merging multiple SSP-RCPs, to increase the number of ensemble members, and then extracting those periods with the same warming level under each SSP. The GCMs and the river model are described in Section 2.1. Similarity in flood projection at the same level of warming among SSP-RCP scenarios was identified by comparing the different SSP-RCPs with respect to flood discharge in the future climate using global distributions and box plots. Then the potential causes of uncertainty among the different SSP-RCPs with respect to the flood change ratio in the future climate was examined. Finally, the ability of our proposed method to reduce the unbiased variance among GCMs with respect to changes in flood discharge in a future climate was determined.

2.1 Flood simulation and runoff data

Flood discharge simulations were performed using the Catchment-based Macro-scale Floodplain Model (CaMa-Flood; Yamazaki et al., 2011) ver. 4.10 (Yamazaki et al., 2022), which efficiently calculates channel flow and floodplain inundation simultaneously. Specifically, it parameterizes the topography of the river channel and floodplain and then calculates the channel and floodplain storage volumes, water depth, inundation area, and water surface gradient in the direction of the downstream grid based on the total storage volume of each grid. Although CaMa-Flood is a river dynamics model for the global domain, it is able to represent the physical processes necessary to reproduce floodplain inundation dynamics. The river network map of CaMa-Flood (6-arcmin resolution in this study) was constructed by upscaling a high-resolution river topographic map (MERIT Hydro; Yamazaki et al., 2019). A detailed description of CaMa-Flood is provided in Yamazaki et al. (2011, 2012, 2014).

In this study, 6-arcmin resolution river simulations were forced with the daily runoff outputs of the GCMs for two time periods: historical (1980-2014) and future (2015-2100). For the latter, three scenarios based on a combination of SSP-RCPs (SSP1-RCP2.6, SSP2-RCP4.5, and SSP5-RCP8.5) were used. GCM-output runoff was converted from its original spatial resolution to 30-arcmin resolution through bilinear interpolation. Nine GCMs from independent institutes were used

(Hirabayashi et al., 2021): MIROC6, IPSL-CM6A-LR, GFDL-CM4, NorESM2-MM, ACCESS-CM2, INM-CM5-0, MPI-ESM1-2-HR, MRI-ESM2-0, EC-Earth3. The experimental setting and other details are given in Table 1.

Table 1: Summary of the experimental set-up, analytical targets, and the figures reporting the results.

Target	At X°C warming	GCM	SSP-RCP	No. of ensemble	Figure
Similarity of the flood hazard under the same warming level among different SSP-RCPs	2°C	ACCESS-CM2 EC-Earth3 IPSL-CM6A-LR	SSP1-RCP2.6 SSP2-RCP4.5 SSP5-RCP8.5	3	Figure1-3 and Figure S1-S4
Potential causes of uncertainty in flood projection among different SSP-RCPs		ACCESS-CM2 EC-Earth3 IPSL-CM6A-LR	SSP1-RCP2.6 SSP2-RCP4.5 SSP5-RCP8.5	3	Figure 4
Quantify the extent to which uncertainty can be reduced by integrating SSP-RCPs.		9GCM	SSP1-RCP2.6 SSP2-RCP4.5 SSP5-RCP8.5	1	Figure 5 and Figure S5
Uncertainty due to GCM climate sensitivity	2°C/3°C	9GCM	SSP5-RCP8.5	1	Figure 6 and Figure S6/S7

2.2 Similarity of the flood hazard under the same warming level among different SSP-RCPs

The similarity in the future flood discharge among the different SSP-RCP was investigated by comparing the spatial distribution of the flood discharge change ratio for each SSP-RCP. The future flood discharge at specific warming levels (SWLs) of X°C above the preindustrial temperature was calculated as follows. As in previous research (Dottori et al., 2018), SWLs were calculated as the year each SWL first surpassed a reference temperature relative to the preindustrial period (1850–1900), using a running mean of the 30-year global averaged annual mean temperature (Supplementary Tables S1). The magnitude of the flood discharge corresponding to the 100-year return period at the SWL (30-year sample including 15 years before and 14 years after the SWL year) was calculated for each catchment using the annual maximum daily discharge fitted to the Gumbel distribution with the L-Moments method (Hosking, 2015). With only 30 samples, the influence of uncertainty due to extreme values may be large. Therefore, multiple ensembles were used and the sample size was increased. Specifically, three ensembles were used in one SSP-RCP (Supplementary Tables S2), and the presence of extreme values was analyzed for 90 samples (30 years x 3 ensembles), by fitting to the Gumbel distribution. The same procedure was used to calculate the flood discharge for the historical period (1980-2014), and then the flood discharge change ratio was calculated using Eq. (1):

$$\frac{(flood\ discharge\ (X°C) - (flood\ discharge\ (historical))}{flood\ discharge\ (historical)} \quad (1)$$

Even for the same GCM and under the same SSP-RCP, the timing of X°C warming may differ between different ensembles, due to internal climate variability. The timing of the 2.0°C warming was therefore investigated in three multiple ensembles of IPSL-CM6A-LR under the same SSP-RCP, which showed a difference of only about 1 year between ensembles. The same was true for other GCMs (ACCESS-CM2 and EC-Earth3) with multiple ensemble experiments under the same SSP-RCP. Those results support the use of the same period for the other ensembles, assuming that the timing of the X°C warming is the same as "r1i1p1f1", which is the first available initial condition ensemble member.

Whether the change trends in each grid are similar across various SSP-RCP scenarios was determined in a global-scale analysis, based on Donnelly et al., 2017. That study compared the differences in runoff, discharge, and related factors between the high-end climate scenario (RCP 8.5) and lower RCPs (RCP2.6 and RCP4.5). Then the flood discharge change ratios between the lower SSP-RCPs and the higher SSP-RCP were compared. Donnelly et al., 2017 also compared the differences in impacts between different warming levels, by plotting the average change attributed to one warming level (e.g., 1.5°C) combined with another level (e.g., 2°C) for each grid point on a scatter plot. The visual presentation of the data was enhanced by summarizing the scatter plot in a box plots diagram, by dividing the x-axis into 30 equally sized bins and showing the y-quartile range for each bin. Likewise, in this study, the flood discharge change ratio from the historical to the future climate was summarized in a box plots diagram.

2.3 Potential causes of uncertainty in flood projections among different SSP-RCPs

The potential causes of uncertainty among the different SSP-RCPs with respect to the flood change ratio in the future climate was analyzed by comparing the spatial distribution patterns of the variation (standard deviation) of the flood change ratio among different ensembles (same GCM under SSP5-RCP8.5) and among different SSP-RCPs (same GCM). If the spatial distribution of variation among different SSP-RCPs of the same GCM was similar to that among the different ensembles, the differences in the pathways of warming to the same temperature increase can be said to be not very large, in terms of the physical changes in flood magnitude under the spatiotemporal resolution covered in this study. In that case, the SSP-RCPs could be treated as ensemble members during the time of X°C warming and thus merged to reduce the uncertainty due to small number of ensemble members. Note that the SSP-RCPs pathway could be crucial for impact assessment items where the irreversibility of future change is significant, such as ecosystem impacts.

2.4 Ability of SSP-RCP integration to reduce the projection uncertainty for future flood hazard

The extent to which integration of the SSP-RCPs could reduce the uncertainty due to small number of ensemble members was quantified by comparing the variability among GCMs with respect to the change in the flood discharge during the historical climate to in response to 2°C warming, first using only SSP5-RCP8.5 and then using our proposed method integrating multiple SSP-RCPs. Unbiased variance is an indicator that allows a comparison of the variance of data derived from different numbers of samples: a lower value indicates reduced uncertainty. In this study, unbiased variance was applied because sample sizes can vary depending on the method used to integrate the SSPs and ensemble members (see Discussion). Warming of 2°C was chosen because it is used in many GCMs and SSP-RCPs.

Our proposed method integrates multiple SSP-RCP into a 90-year (or 60-year) time-series data set at each GCM and then performs an extreme values analysis. The procedure involves the following: (1) A survey of the nine GCMs and three SSP-RCPs to identify those that reach 2.0°C (Supplementary Table S1), which in this study yielded 21 GCM-SSP-RCPs. (2) Calculation of the flood discharge using multiple SSP-RCPs in one GCM and increasing the sample size (i.e., number of years) to mitigate the uncertainty due to extreme values. Specifically, three (or two) SSP-RCPs were used in one GCM, and an extreme value analysis was performed for 90-year (or 60-year) time-series data; flood discharge under the future climate was calculated in each GCM. For example, in the case of three SSP-RCPs in one GCM, the extreme value analysis performed for the annual maximum discharge for 90 years = 30 years × 3 SSP-RCPs). (3) Performing an extreme value analysis for the annual maximum discharge during the historical climate (1980-2014) according to each GCM to calculate the flood discharge and flood change ratio at 2°C warming for each GCM using Eq. (1). (4) Calculation of the unbiased variance of the flood change ratio among the nine GCMs at each grid point.

3 Results

3.1 Similarity in the flood projection at the same warming level among SSP-RCPs

The spatial distribution of the flood discharge change ratio from the historical climate to 2°C warming in IPSL-CM6A-LR showed similar patterns among the different SSP-RCPs (Figure 1). In all of them, flooding increased in many areas in Southeast Asia and low-latitude Africa, while it decreased from northern and eastern Europe to western Russia, in central North America, and in northern South America. Thus, the differences among SSP-RCP scenarios were relatively small in comparisons of the flood change at a specific degree of global warming. The same analyses for EC-Earth3 and ACCESS-CM2 showed similar results (Supplementary Figs. S1, S2).

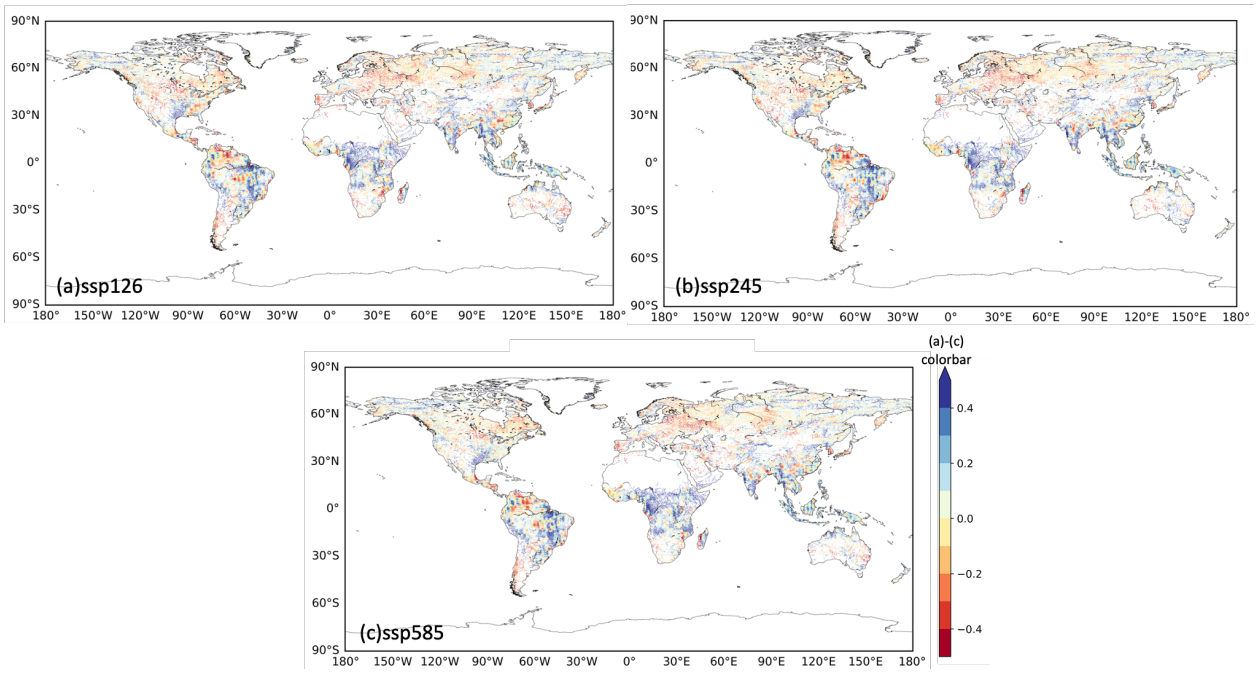

Figure 2: Spatial distribution of the flood change ratio from the historical climate to 2°C warming for each SSP-RCP of IPSL-CM6A-LR: (a) SSP1-RCP2.6, (b) SSP2-RCP4.5, (c) SSP5-RCP8.5. Grid cells with a flood discharge in the historical climate < 100 m3/s were excluded.

In the quantitative analysis, conducted at a global scale, box plots were used to diagram whether the trend of a change in each grid was similar between different SSP-RCP scenarios. Figure 2 shows the flood change rate at the same warming level obtained from different SSP-RCPs in IPSL-CM6A-LR. The median value of the bins is located around y=x, indicating that flood discharge is similar (differences of 5–10%) at the same warming level regardless of the SSP-RCP. Figure 3 shows the flood change ratio for the different warming levels in IPSL-CM6-LR. For all SSP-RCPs, there was a tendency for increased floods with warmer temperatures. For example, the flood change ratio in most of the grid cells is larger for 3.0 than for 2.0 and the slope "b" of the fitted line of the flood change ratio was 1.28. The value of "b" was similar for 1.5 and 2.0 whereas for 3.0 and 4.0 the magnitude of the difference in the flood change ratio between different warming levels was 20-30%, which was larger than the difference among different SSP-RCPs at the same warming level.

A comparison of the box plots for ACCESS-CM2 and EC-Earth3 is shown in Supplementary Figs. S3 and S4. For EC-Earth3 (Supplementary Fig. S3) the trend was the same as in Figure 2, but a future flood hazard difference between different SSP-RCPs was suggested by ACCESS-CM2 (Supplementary Fig. S4), perhaps because the response of flood discharge to the same warming level may vary depending on SSP-RCPs. Other possible factors contributing to the difference include the following: (1) A 90-year annual maximum discharge may not be long enough for extreme value analysis to evaluate a flood discharge corresponding to a 100-year return period, such that uncertainty remains. (2) Uncertainty surrounds projections for low warming and near-term scenarios (e.g., 2°C warming) (Maher et al., 2020), with the possibility of substantial uncertainty

due to internal climate variability. (3) The extreme value analysis was performed by extracting the 30-year moving average, so that scenarios such as SSP5-RCP8.5, in which temperatures increase rapidly, include years when warming is higher (or lower) than 2°C warming, in contrast to SSP1-RCP2.6/SSP2-RCP4.5, and there may be a difference in the range of temperature increases.

The above results showed that future flood changes in hazards, such as flood discharge, differ between different SSP-RCPs, but the differences are smaller than those between different warming levels. Although trends may vary by GCM, integrating different SSP-RCPs may reduce the uncertainty due to small number of ensemble members. In the next section, we analyzed the causes of uncertainty among different SSP-RCPs in the flood discharge of a future climate, by examining the spatial distributions of the standard deviations.

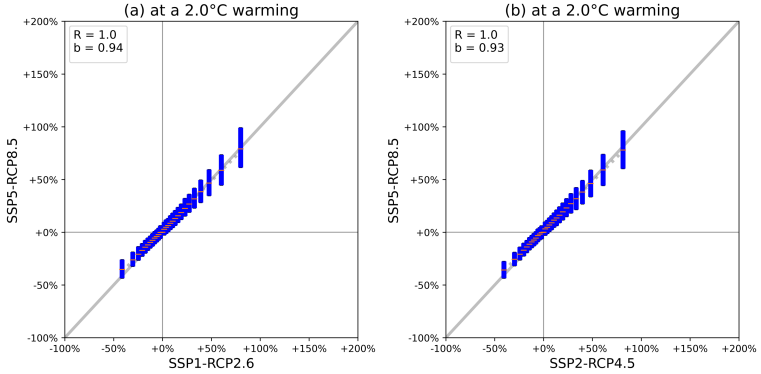

Figure 2: Comparison of the flood change ratio among two future scenarios characterized by the same warming level but under different RCP-SSP scenarios: (a) 2.0°C warming between SSP1-RCP2.6 and SSP5-RCP8.5; (b) 2.0°C warming between SSP2-RCP4.5 and SSP5-RCP8.5 (IPSL-CM6-LR). The dashed line is a linear fit (least squares) through the origin to the bin median values; "b" is the slope of the fitted line and the R value is the correlation coefficient.

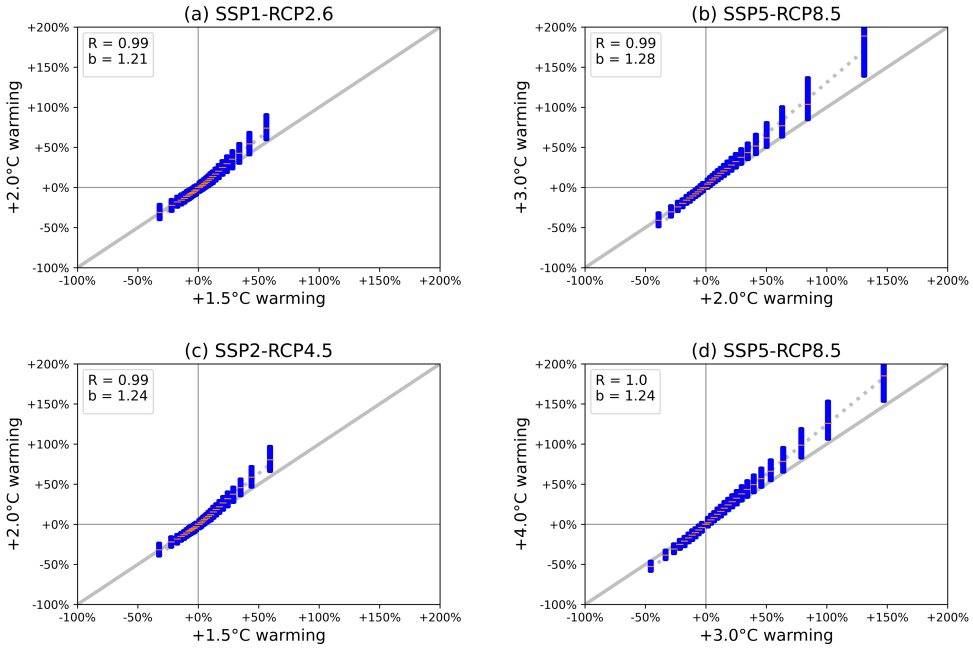

Figure 3: Comparison of the flood change ratio among two future scenarios at different warming levels: (a) 1.5°C and 2.0 °C under SSP1-RCP2.6; (b) 2.0°C and 3.0 °C under SSP5-RCP8.5; (c) 1.5°C and 2.0°C under SSP2-RCP4.5; (d) 3.0°C and 4.0 °C under SSP5-RCP8.5 (IPSL-CM6-LR). The dashed line is a linear fit (least squares) through the origin to the bin median values; "b" is the slope of the fitted line and the R value is the correlation coefficient.

3.2 Potential causes of uncertainty in flood projections among SSP-RCPs

To investigate the causes of uncertainty among different SSP-RCPs with respect to flood discharge in a future climate, the global spatial distribution of the variability (standard deviation) in the flood change ratio from the historical climate to 2.0°C warming was compared among different SSP-RCPs of the same GCM and among different ensembles of the same GCM under SSP5-RCP8.5 (Figure 4). Figure 4(a) shows the large variability and thus the large uncertainty in the same regions, including the Mississippi River (USA), the low-latitude region of Africa, and the region extending from China across Southeast Asia.

The main source of the variation among different ensembles of the same GCM under the same SSP-RCP is internal climate variability. This variation had a similar spatial distribution as in Fig. 4b, which implies that the main source of the difference among SSP-RCPs was internal climate variability. Thus, the differences in the pathways of warming to the same temperature increase can be said to be not very large, in terms of the physical changes in flood magnitude under the spatiotemporal resolution covered in this study. As noted above, integrating different SSP-RCPs may reduce the uncertainty due to small number of ensemble members.

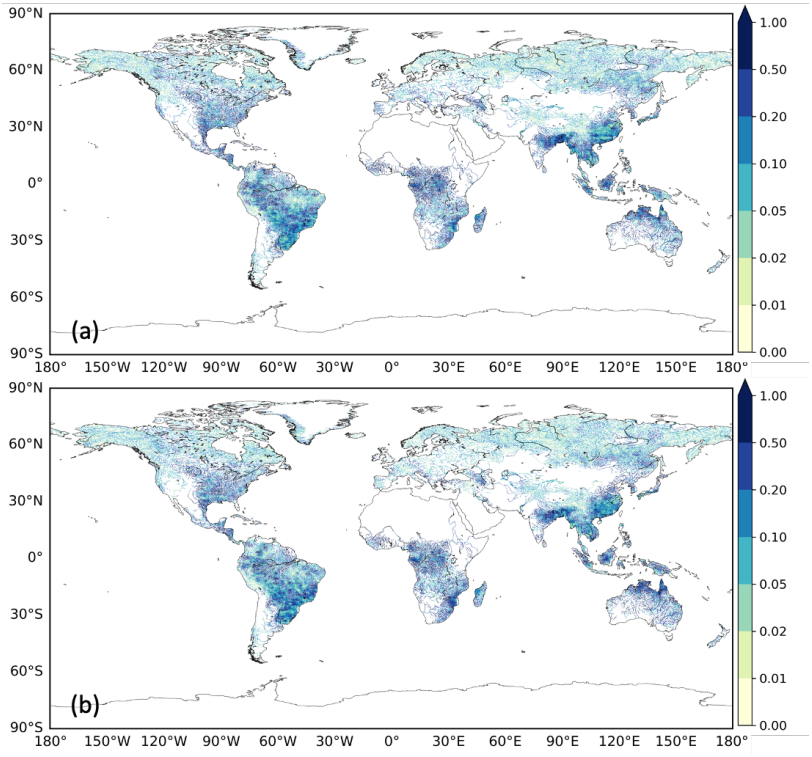

Figure 4: The global spatial distribution of the standard deviation of the flood change ratio from the historical climate to 2.0°C warming (IPSL-CM6-LR). (a) Standard deviation among three different SSP-RCPs; (b) standard deviation among three different ensembles (SSP5-RCP8.5). Grid cells with a 100-year RP discharge in the historical climate < 100 m3/s were excluded.

3.3 Reduction of uncertainty in flood projection by the proposed method

The results of Figures 1-4 show that the uncertainty in the flood projection could be reduced using our proposed method. The uncertainty in flood projection using our method was reduced in approximately 70% of the grid points compared to when the simulation was performed only with SSP5-RCP8.5 (Figure 5). This pattern was particularly evident in grid points in which the unbiased variance among GCMs was larger than 0.1. Specifically, unbiased variance significantly decreased in the Mississippi River (USA) and from China to Southeast Asia. These results suggest that the uncertainty in flood hazard projection can be reduced by our method. However, even after integrating multiple SSP-RCPs, regions with large unbiased variance among GCMs remained, indicating a large uncertainty, including differences in the physical parameters of climate models.

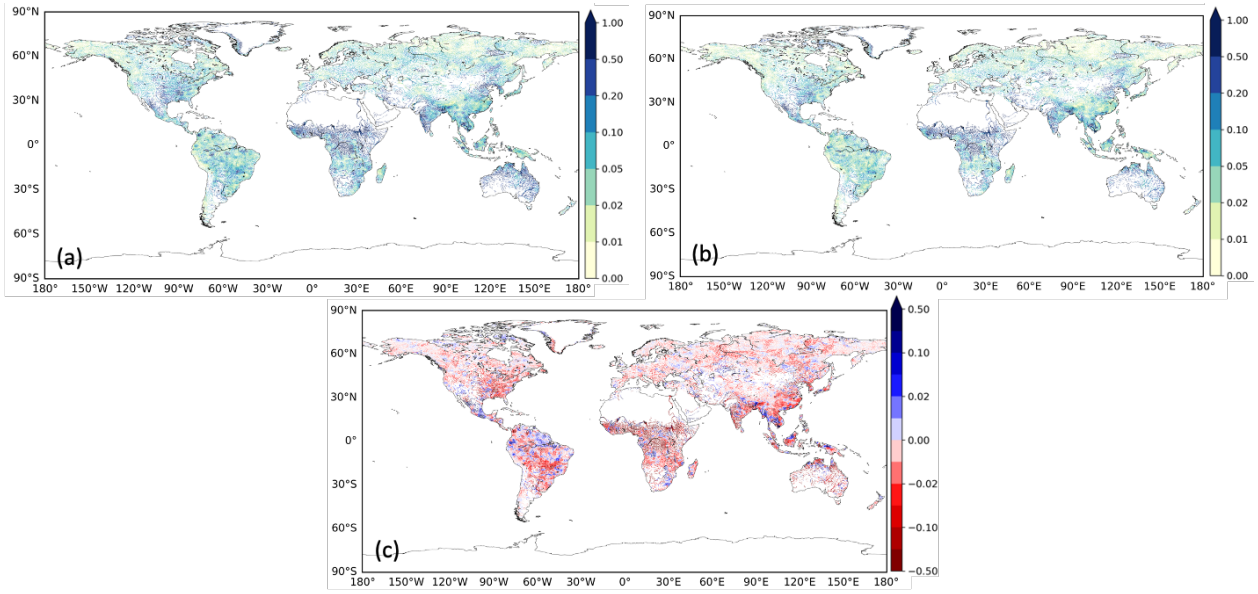

Figure 5: Unbiased variance in the flood change ratio from the historical climate to 2.0°C warming (a) among nine GCMs (only SSP5-RCP8.5) and (b) among nine GCMs integrating multiple SSP-RCP into a 90-year (or 60-year) time-series data set at each GCM, performing an extreme value analysis and calculating unbiased variances. (c) Change in the variance from (a) to (b) are also shown.

.

4 Discussion

4.1 Alternative method for integrating multiple SSP-RCPs

In our proposed method, multiple SSP-RCPs are integrated into a 90-year (or 60-year) time-series data set at each GCM after which extreme parameters are calculated to reduce uncertainties in flood hazard projection. The advantages of our method are that the sample size is increased for extreme value estimation and the uncertainty due to small number of ensemble members is reduced. In this section, we present another method for multiple SSP-RCP integration, in which extreme parameters are calculated individually from a 30-year sample for each SSP-RCP followed by a calculation of the unbiased variance in the flood change. The method is described in detail in Supplementary Text S1.

The uncertainty in flood projection using the alternative method to integrate multiple SSP-RCPs is reduced in only approximately 50% of the grid points, in contrast to when only SSP5-RCP8.5 is used (Fig. 6 and Supplementary Fig. S5). There are a couple of possible reasons for this. It may be due to the impact of uncertainty in extreme value analysis due to a small sample size; i.e., a 30-year sample of annual maximum daily discharge may not be sufficient for extreme value analysis in the evaluation of flood with a 100-year return period, such that uncertainty remains. In addition, uncertainty surrounds projections for low warming and near-term scenarios (e.g., 2°C warming) (Maher et al., 2020), with the possibility of substantial uncertainty due to internal climate variability. Increasing the sample size without reducing the uncertainty of

each GCM-SSP may not reduce the variability among GCMs. Our results demonstrate the importance of integrating the SSP-RCP prior to the extreme value analysis to reduce the uncertainty due to small number of ensemble members

4.2 Comparison with an analysis focused on a specific time period

Several studies (e.g., Hirabayashi et al., 2021; Kimura et al., 2023; Winsemius et al., 2016) have investigated the effects of flood hazard and risk during a specific time period (e.g., end of the 21st century). The information can be applied to support policy-linked actions. However, because each GCM has a different warming level at a specific time period, it is subject to uncertainties due to differences in climate sensitivity. In this section, the impact of those uncertainties is examined. Details of the method are provided in Supplementary Text S2.

The unbiased variance among the nine GCMs at 3°C warming was smaller than that among the nine GCMs in 2064, when the mean temperature increase predicted by those GCMs is 3°C. This difference can be explained by variation in climate sensitivity among the models. Compared to 2064, the evaluation at 3°C warming showed a reduction in unbiased variance in approximately 70% of the land grid points (Figure 6 and Supplementary Fig. S6). This reduction was more pronounced, reaching around 80% of the grid points, in regions characterized by an initially substantial unbiased variance between GCMs. The reductions were mostly in the low-latitude regions of Africa and the region extending from China to Southeast Asia. Grid points with an increase in unbiased variance were those in the Amazon River basin, perhaps due to the different change trends in the different SSP-RCP scenarios around the Amazon River. Supplementary Fig. S1 shows the different change trends for each SSP-RCP in the Amazon region.

Compared to 2042, the evaluation at 2°C warming showed a reduction in unbiased variance in only approximately 50% of the land grid points; both increases and decreases were detected (Figure 6 and Supplementary Fig. S7). These results may reflect the uncertainty surrounding precipitation projections for the near-term period with a lower level of warming. This uncertainty arises from natural internal climate variability, model uncertainty, and uncertainty in natural and anthropogenic aerosol forcing.

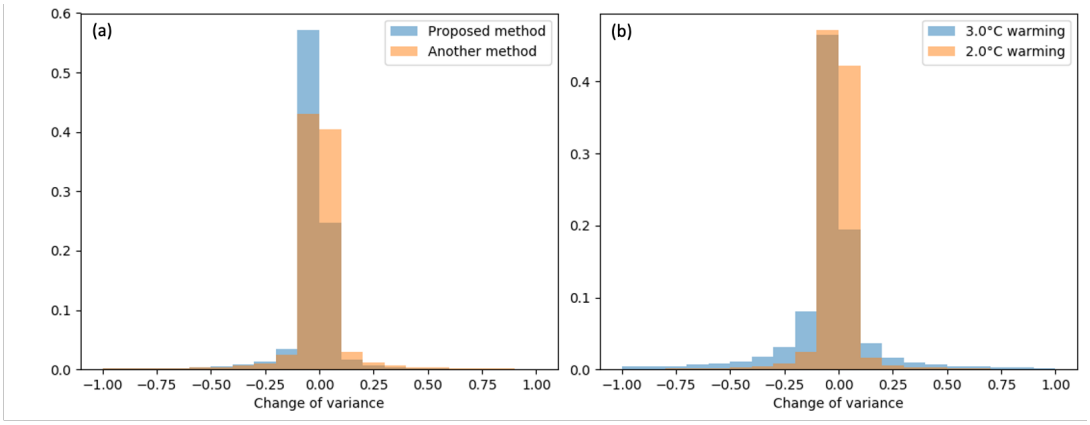

Figure 6: Histogram showing (a) the change in unbiased variance among nine GCMs using only SSP5-RCP8.5 vs. the proposed method (blue) or the alternative method (orange). (b) The change in unbiased variance among nine GCMs between a particular future year (2064 or 2042) under SSP5-RCP8.5 and the evaluation at 3.0°C (blue) or 2.0°C (orange) of warming in each GCM. Note that the unbiased variance among the nine GCMs is defined based on 100-year RP discharge change ratio from the historical climate.

4.3 Uncertainty in flood risk estimation

The variability (unbiased variance) among GCMs can be reduced by performing an extreme value analysis after integrating the annual maximum discharges of multiple SSP-RCPs for each GCM. In this section, this approach, carried out according to our proposed method, is used to analyze the changes in flood risk (exposed population and GDP) with each warming level. The future climate inundation depth distribution was constructed based on the change in future flood frequency at X°C warming, using the lookup method of Kimura et al., 2023. Detailed explanations of the construction of a future flood hazard map and of the population and GDP data used in this section are provided in Supplementary Text S3.

Figure 7 and Supplementary Table S3 show the impacts on both the population and GDP based on the distribution of future inundation depths at X°C warming. The affected population was predicted to be 1.62 billion under the historical climate and 1.69-1.79 billion in the case of 1.5-4°C warming according to the future climate hazard map, an increase of 4-10%. The affected population under the historical climate in particularly high-risk areas (flood depth ≥ 5 m) was predicted to be 0.243 billion and in a future climate with a 1.5-4°C warming 0.292-0.368 billion, an increase of 20-51%. The affected GDP was USD 21.1 trillion under the historical climate and USD 21.8-22.7 trillion in the case of 1.5-4°C warming, an increase of 3-7%. The affected GDP in the particularly high-risk areas (flood depth ≥ 5 m) was 3.1 USD trillion under the historical climate and 3.6-4.3 USD trillion in a scenario with 1.5–4°C warming, an increase of 14–38%. Thus, in areas at particularly high risk subsequent to X°C warming, the affected population and affected GDP are significantly higher.

Next, we investigated whether the proposed method reduces the uncertainty in future impact assessments. To this end, future hazard maps based on the change in flood frequency for each GCM were created using the lookup method; we compared the use of only the SSP5-RCP8.5 scenario to the use of our new method. Then the affected population in each case at X°C warming was determined to estimate the magnitude of the reduction of uncertainty in future impact assessments that could be achieved using the proposed method.

Table 2 shows the change in the size of the affected population at X°C warming compared to the historical climate after applying the two approaches described above. The proposed method reduced the variation among the nine GCMs with respect to the affected population by 8-10%, thus demonstrating its ability to reduce the uncertainty in future flood impact assessments.

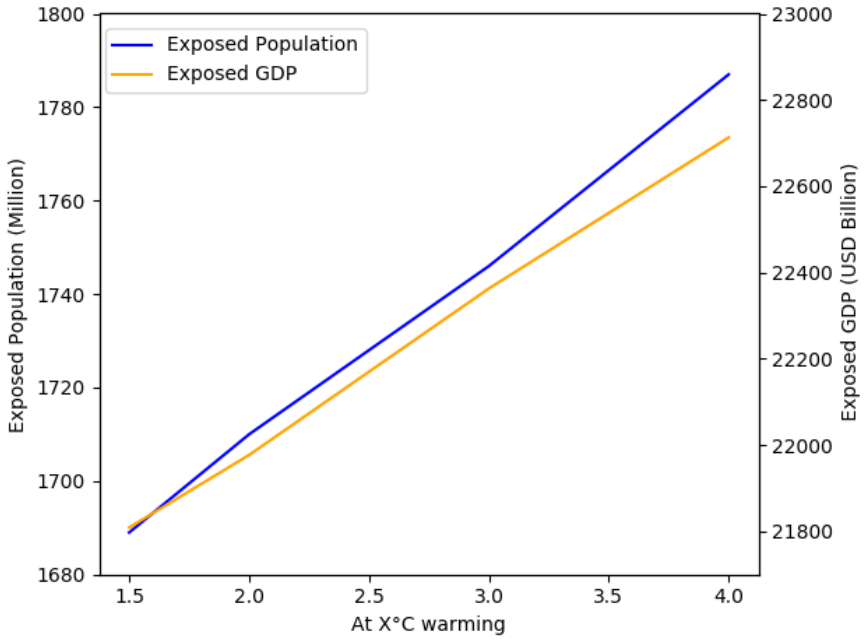

Figure 7: Line graph showing the affected population (blue) and affected GDP (orange) within the inundation area of the 100-year RP hazard map and at X°C warming.

Table 2: Change in the affected population at X°C warming vs. the historical climate according to the two approaches based on the lookup method. (unit : million).

	At 2°C warming		At 3°C warming	
	9GCM average	Unbiased Variance among 9GCM	9GCM average	Unbiased Variance among 9GCM
(1)Using only SSP5-RCP8.5	+61	39	+80	34
(2) Using our proposed method	+56	36	+83	31
Change ratio from (1) to (2)		-7.9%		-9.7%

4.4 Study Limitations

The similarity in flood projection at a same level of warming among SSP-RCP scenarios was investigated, with the RP-100 year flood discharge calculated by extreme value analysis using 90 years of data from three ensemble members. However, a larger number of ensembles would have allowed more precise determination of the uncertainty. In addition, although integrating multiple SSP-RCPs was effective, the optimal number of ensembles to sufficiently reduce uncertainty must also be determined, as pointed out by Shiogama et al., 2023.

The uncertainty in climate change predictions of river discharge was also examined using the daily runoff output of the GCMs, without bias correction. Relative future changes instead of absolute values were used based on the assumption that the bias structure was consistent between historical and future scenarios. This allowed the use of the lookup method to estimate the flood hazard under a future climate (Kimura et al., 2023). The lookup method does not require bias correction; rather, it allows calculation of the frequency change under the future climate from the GCMs, with the result then combined with the reanalysis data. However, we did not consider factors beyond climate change, such as human activities, which have a significant impact on river discharge.

Our method is based on the assumption that SSP-RCP results are similar for the same temperature rise. In Section 3.1, we showed that this assumption was reasonable. A similar method that utilizes this approach has been proposed; for example, a system that extracts the results of future predictions by GCMs at a specific temperature rise timing (Tebaldi et al., 2022). While this study demonstrates that the method is suitable for monthly average precipitation and temperature, this study shows that a similar method can be applied to extreme events such as flooding. However, for GCM experiments conducted under significantly different conditions described by other scenarios, with variation in factors beyond greenhouse gas concentrations, additional analysis is needed to confirm that the results for the same temperature rise in the GCM do not differ substantially among SSP-RCPs scenarios. For example, the characteristics of SSP3-RCP7.0 are distinct from those of the other scenarios. Aerosol emissions increase only slightly in SSP3-RCP7.0, due to the assumption of lenient air quality policies, but they decrease in the other SSP-RCPs and all of the RCPs (Lund et al., 2019). While the global mean temperature projection of SSP3-RCP7.0 is between that of SSP2-RCP4.5 and SSP5-RCP8.5, the global mean change in precipitation in SSP3-RCP7.0 is similar to that of SSP2-RCP4.5, due to the influence of aerosols, which in the latter is 39% less than in scenarios with the same radiation forcing as SSP3-RCP7.0 but with lower aerosol emissions (Shiogama et al., 2023).

We anticipate that our method can be applied to variables other than flood discharge, but this remains to be verified. A first step would be to confirm that there is little difference between SSP-RCPs for each variable, although some studies have investigated the differences and similarities in climatic hazards projection (e.g., precipitation, runoff, glacier) at the same level of warming as among SSP-RCP scenarios (e.g., Donnelly et al., 2017, Liu et al., 2021). In their study of precipitation and runoff, Donnelly et al., 2017 showed that the differences among SSP-RCP scenario at the same warming level are

generally smaller than those between different warming levels. This result provides support for our method of integrating SSP-RCPs to estimate precipitation and runoff.

5 Conclusions

This study investigated whether the uncertainty in future flood prediction due to small number of ensemble members could be reasonably reduced by merging multiple SSP-RCPs and extracting the periods with the same warming level under each SSP-RCP. The uncertainty due to small number of ensemble members is a one of the major source of uncertainty in future climate predictions. Projection uncertainty due to the above could be mitigated by increasing the number of ensembles. However, only a limited number of large-ensemble experiments are available for each of the CMIP6 GCMs. Therefore, while increasing the ensemble size may be difficult, evaluating the hazard of X°C warming by integrating multiple SSP-RCP with data at the time of that warming may increase the sample size. This study investigated whether the uncertainty in future flood prediction due to small number of ensemble members could be reasonably reduced by merging multiple SSP-RCPs and extracting those periods with the same warming level under each SSP-RCP.

A preliminary investigation of the similarity in flood projection at the same level of warming among SSP-RCP scenarios showed that at 2°C warming the change ratio in the flood magnitude showed similar distributions for all SSP-RCPs. Moreover, the uncertainty due to the different SSP-RCPs (5-10%) was smaller than the difference in flood hazard between 2°C and 3°C or between 3°C and 4°C (20-30%), which suggests that differences among SSP-RCPs as to future flood discharge change are relatively small. Accordingly, integrating multiple SSP-RCPs is an appropriate method for reducing the uncertainty due to small number of ensemble members in impact assessments at X°C warming.

The ability of our method to reduce the variability among GCMs regarding future flood changes in hazards was compared to the use of SSP5-RCP8.5 alone. The unbiased variance among GCMs in our method was reduced in about 70% of the grid points compared to when SSP5-RCP8.5 alone was applied. In regions characterized by an initially significant unbiased variance among GCMs, the reduction increased to about 80% of the grid points, with significant decreases in the Mississippi River (USA) and extending from China to Southeast Asia.

Finally, the proposed method was tested by creating future hazard maps based on the change in flood frequency in each GCM using the lookup method with only nine GCMs under the SSP5-RCP8.5 scenario vs. using the proposed method. Then the size of the affected population at X°C warming was calculated according to these two approaches. The results showed a reduction in the variation among GCMs of the affected population of 8-10%.

Based on the above results, our proposed method is very helpful for assessing climate change impacts because it could not only meet the growing need to evaluate impacts of specific warming levels but also reduce the uncertainty as to future flood impact assessment. The proposed method is expected to be commonly used as a method to reduce the uncertainty of small

number of ensemble members regarding future projections in CMIP6 and to provide a more accurate estimates of the impacts of climate change.

Code availability

The global hydrodynamic model CaMa-Flood (v4.10) is available from (https://zenodo.org/records/7597409) (Yamazaki et al,. 2022).

Data availability

The topography data MERIT are available from http://hydro.iis.u-tokyo.ac.jp/~yamadai/MERIT_DEM/index.html (last access: 17 August 2023) (Yamazaki et al., 2019).

The CMIP6 data are available from the Earth System Grid Federation (ESGF) data platform (https://esgf-node.llnl.gov/search/cmip6/, accessed on 17 August 2023).

Author contribution

Y. Kimura, Y. Hirabayashi and D. Yamazaki conceived the study and contributed to the development and design of the methodology. Y. Kimura performed simulation and analysis. Y. Kimura and D. Yamazaki prepared the manuscript with review from Y. Hirabayashi.

Acknowledgements

This research was supported by LaRC-Flood Project co-funded by MS&AD and NEDO (JP21500379). This research was partially supported by MEXT “Program for the advanced studies of climate change projection” (SENTAN: JPMXD0722680395)

References

Alfieri, L., Bisselink, B., Dottori, F., Naumann, G., de Roo, A., Salamon, P., Wyser K, and Feyen, L(2017), Global projections of river flood risk in a warmer world. Earth's Future, 5(2), 171-182. https://doi.org/10.1002/2016EF000485.

Brêda, J. P. L. F., de Paiva, R. C. D., Collischon, W., Bravo, J. M., Siqueira, V. A., and Steinke, E. B. (2020), Climate change impacts on South American water balance from a continental-scale hydrological model driven by CMIP5 projections. Climatic Change 159, 503–522. https://doi.org/10.1007/s10584-020-02667-9

Cheng D, Shimizu K, Yamada TJ. (2021), Hydrological frequency analysis of large-ensemble climate simulation data using control density as a statistical control. Hydrological Research Letters 15: 84–91. https://doi.org/10.3178/hrl.15.84

Dai, A., Bloecker, C.E. (2019), Impacts of internal variability on temperature and precipitation trends in large ensemble simulations by two climate models. Clim Dyn 52, 289–306. https://doi.org/10.1007/s00382-018-4132-4.

Dankers, R., Arnell, N. W., Clark, D. B., Falloon, P. D., Fekete, B. M., Gosling, S. N., Heinke, J., Kim, H., Masaki, Y., Satoh, Y., Stacke, T., Wada, Y., and Wisser, D. (2014), First look at changes in flood hazard in the inter-sectoral impact model intercomparison project ensemble, P. Natl. Acad. Sci. USA, 111, 3257–3261, https://doi.org/10.1073/pnas.1302078110.

Donnelly, C., Greuell, W., Andersson, J. et al. (2017). Impacts of climate change on European hydrology at 1.5, 2 and 3 degrees mean global warming above preindustrial level. Climatic Change, 143, 13-26., https://doi.org/10.1007/s10584-017-1971-7

Dottori, F., Szewczyk, W., Ciscar, J. C., Zhao, F., Alfieri, L., Hirabayashi, Y., Bianchi, A., Mongelli, I., Frieler, K., Betts R, A. and Feyen., L.(2018), Increased human and economic losses from river flooding with anthropogenic warming. Nature Climate Change, 8.9, 781-786, https://doi.org/10.1038/s41558-018-0257-z.

Eyring, V., Bony, S., Meehl, G. A., Senior, C. A., Stevens, B., Stouffer, R. J., and Taylor, K. E.(2016), Overview of the Coupled Model Intercomparison Project Phase 6 (CMIP6) experimental design and organization. Geoscientific Model Development, 9.5, 1937-1958, https://doi.org/10.5194/gmd-9-1937-2016.

Hirabayashi, Y., Tanoue, M., Sasaki, O., Zhou, X., and Yamazaki, D.(2021), Global exposure to flooding from the new CMIP6 climate model projections. Scientific reports, 11.1, 1-7, https://doi.org/10.1038/s41598-021-83279-w

Hosking, J. R. M.(2015), L-Moments, in: Wiley StatsRef: Statistics Reference Online, John Wiley & Sons, Ltd., Hoboken, USA, 1–8, https://doi.org/10.1002/9781118445112.stat00570.pub2.

Ishii M, Mori N. (2020), d4PDF: Large-ensemble and highresolution climate simulations for global warming risk assessment. Progress in Earth and Planetary Science 7: 58. https://doi.org/10.1186/s40645-020-00367-7

Kimura, Y., Hirabayashi, Y., Kita, Y., Zhou, X., and Yamazaki, D. (2023), Methodology for constructing a flood-hazard map for a future climate. Hydrology and Earth System Sciences, 27(8), 1627-1644., https://doi.org/10.5194/hess-27-1627-2023

Kita, Y., and Yamazaki, D. 2023, Uncertainty of internal climate variability in probabilistic flood simulations using d4PDF. Hydrological Research Letters, 17(2), 15-20. https://doi.org/10.3178/hrl.17.15

Lehner, F., Deser, C., Maher, N., Marotzke, J., Fischer, E. M., Brunner, L., Knutti, R., and Hawkins, E. (2020), Partitioning climate projection uncertainty with multiple large ensembles and CMIP5/6. Earth System Dynamics, 11, 491-508. https://doi.org/10.5194/esd-11-491-2020

Liu, L., Zhao, D., Wei, J., Zhuang, Q., Gao, X., Zhu, Y., Zhang, J., Guo, C., and Zheng, D. (2021). Permafrost sensitivity to global warming of 1.5° C and 2° C in the Northern Hemisphere. Environmental Research Letters, 16(3), 034038., DOI:10.1088/1748-9326/abd6a8

Lund, M. T., Myhre, G., and Samset, B. H. (2019), Anthropogenic aerosol forcing under the Shared Socioeconomic Pathways, Atmos. Chem. Phys., 19, 13827–13839, https://doi.org/10.5194/acp-19-13827-2019.

Maher, N., Milinski, S., and Ludwig, R. (2021), Large ensemble climate model simulations: introduction, overview, and future prospects for utilising multiple types of large ensemble. Earth System Dynamics, 12(2), 401-418., https://doi.org/10.5194/esd-12-401-2021

Mizuta R, Murata A, Ishii M, Shiogama H, Hibino K, Mori N, Arakawa O, Imada Y, Yoshida K, Aoyagi T, Kawase H, Mori M, Okada Y, Shimura T, Nagatomo T, Ikeda M, Endo H, Nosaka M, Arai M, Takahashi C, Tanaka K, Takemi T, Tachikawa Y, Temur K, Kamae Y, Watanabe M, Sasaki H, Kitoh A, Takayabu I, Nakakita E, Kimoto M. (2017), Over 5000 years of ensemble future climate simulations by 60-km global and 20-km regional atmospheric models. Bulletin of the American Meteorological Society 98: 1383–1398. DOI: 10.1175/BAMS-D-16-0099.1.

O'Neill, B. C., Tebaldi, C., van Vuuren, D. P., Eyring, V., Friedlingstein, P., Hurtt, G., Knutti, R., Kriegler, E., Lamarque, J.-F., Lowe, J., Meehl, G. A., Moss, R., Riahi, K., and Sanderson, B. M.(2016), The Scenario Model Intercomparison Project (ScenarioMIP) for CMIP6, Geosci. Model Dev., 9, 3461–3482, https://doi.org/10.5194/gmd-9-3461-2016.

Piao, J., Chen, W. & Chen, S. (2021), Sources of the internal variability-generated uncertainties in the projection of Northeast Asian summer precipitation. Clim Dyn 56, 1783–1797. https://doi.org/10.1007/s00382-020-05557-z

Schwarzwald, K., & Lenssen, N. (2022). The importance of internal climate variability in climate impact projections. Proceedings of the National Academy of Sciences, 119(42), e2208095119, https://www.pnas.org/doi/10.1073/pnas.2208095119

Shiogama, H., Tatebe, H., Hayashi, M., Abe, M., Arai, M., Koyama, H., Imada, Y., Kosaka, Y., Ogura, T., and Watanabe, M.(2023), MIROC6 Large Ensemble (MIROC6-LE): experimental design and initial analyses, Earth Syst. Dynam. Discuss. [preprint], https://doi.org/10.5194/esd-2023-12, in review.

Tebaldi, C., Snyder, A., & Dorheim, K. (2022). STITCHES: creating new scenarios of climate model output by stitching together pieces of existing simulations. Earth System Dynamics, 13(4), 1557-1609. https://doi.org/10.5194/esd-13-1557-2022

Ward, P. J., Kummu, M., & Lall, U. (2016). Flood frequencies and durations and their response to El Niño Southern Oscillation: Global analysis. Journal of Hydrology, 539, 358-378. https://doi.org/10.1016/j.jhydrol.2016.05.045

Winsemius, H., Aerts, J., van Beek, L. et al. (2016). Global drivers of future river flood risk. Nature Climate Change, 6(4), 381-385., https://doi.org/10.1038/nclimate2893

Wood, R. R., and Ludwig, R. (2020), Analyzing internal variability and forced response of subdaily and daily extreme precipitation over Europe. Geophysical Research Letters, 47(17), https://doi.org/10.1029/2020GL089300.

Yamazaki, D., Kanae, S., Kim, H., and Oki, T.(2011), A physically based description of floodplain inundation dynamics in a global river routing model. Water Resources Research, 47.4, https://doi.org/10.1029/2010WR009726.

Yamazaki, D., Lee, H., Alsdorf, D. E., Dutra, E., Kim, H., Kanae, S., and Oki, T.(2012), Analysis of the water level dynamics simulated by a global river model: A case study in the Amazon River, Water Resour. Res., 48, 1–15, https://doi.org/10.1029/2012WR011869.

Yamazaki, D., Sato, T., Kanae, S., Hirabayashi, Y., and Bates, P. D.(2014), Regional flood dynamics in a bifurcating mega delta simulated in a global river model. Geophysical Research Letters, 41.9, 3127-3135, https://doi.org/10.1002/2014GL059744.

Yamazaki, D., Ikeshima, D., Sosa, J., Bates, P. D., Allen, G. H., and Pavelsky, T. M.(2019), MERIT Hydro: A high-resolution global hydrography map based on latest topography dataset. Water Resources Research, 55.6, 5053-5073, https://doi.org/10.1029/2019WR024873.

The English in this document has been checked by at least two professional editors, both native speakers of English. For a certificate, please see: http://www.textcheck.com/certificate/ZwVi4C